

**EFFECT OF PULSED LASER ABLATION ON THE INCREASE
OF ADHESION OF CRN COATING-SUBSTRATE**

¹Paulína ZACKOVÁ, Lucia ŠTEVLÍKOVÁ, Ľubomír ČAPLOVIČ,
Martin SAHUL, ²Vitali PODGURSKI

¹SLOVAK UNIVERSITY OF TECHNOLOGY IN BRATISLAVA,
FACULTY OF MATERIALS SCIENCE AND TECHNOLOGY IN TRNAVA,
INSTITUTE OF MATERIALS SCIENCE,
ULICA JÁNA BOTTU 2781/25, 917 24 TRNAVA, SLOVAK REPUBLIC
e-mail: paulina.zackova@stuba.sk, lucia.stevlikova@stuba.sk, lubomir.caplovic@stuba.sk,
martin.sahul@stuba.sk

²TALLINN UNIVERSITY OF TECHNOLOGY,
DEPARTMENT OF MECHANICAL AND INDUSTRIAL ENGINEERING,
EHITAJATE TEE 5, 19086 TALLINN, ESTONIA
Received 27 August 2018, accepted 19 October 2018, published 27 November 2018

Abstract

The contribution deals with analysis of the influence of the substrate surface laser ablation before deposition process to improve the adhesion of coating-substrate system. The coatings were applied to the high-speed steel 6-5-2-5 (STN 19 852) and WC-Co cemented carbide with cobalt content of 10 wt%. Lateral Rotating Cathodes (LARC[®]) process was chosen for evaporation of individual CrN layers. Influence of laser ablation on the substrate morphology, structure, roughness, presence of residual stresses inside the substrates and layers and their adhesion behavior between the layers and the base material was studied. Scanning electron microscopy fitted with energy dispersive spectroscopy was utilized to investigate morphology and fracture areas of substrates with CrN layers. X-ray diffraction analysis was employed to detect the residual stresses measurements. Adhesion between the coatings and substrate was analyzed using “Mercedes” testing.

Key words

CrN coatings, laser ablation, substrate surface, Scanning electron microscopy, adhesion, residual stresses

INTRODUCTION

There are many conventional methods of chemical-heat treatment which allow producing thin coatings of special properties on the surface of metallic materials. They are currently

associated with the new methods of functional layers formation, which allow, to a certain extent, to solve problems of short lifetime and reliability of tools and mechanically stressed components. Lifetime of a tool depends on its quality, material it is made of, and its surface treatment. Coatings applied to steels and other metallic materials offer exceptionally good tribological properties in many applications. In particular, it is low friction coefficient, wear resistance, but also an improvement of corrosion and chemical resistance and high surface hardness that increase the lifetime of tools and components (1, 2). However, it is necessary to understand the coatings as a coating-substrate system, since only within the system the layer of a given thickness achieves specific behavior and properties. Therefore, one of the most important criteria for the proper functioning of this system is the adhesion between the coating and the base material. The problem of low adhesion can be successfully addressed by treatment of the substrate surface before the coating deposition. It is, for example, etching - removing cobalt from the surface of the sintered carbides used as a base material, water jetting, surface roughening by diamond powder using the adhesive interlayer and others (3-5). An important procedure for surface treatment of the substrate prior to deposition of the PVD coating is an application of laser radiation, i.e. laser ablation. Laser surface modification of the substrate may also include adjustment of the surface topography, which is important for the adhesion of the subsequently deposited coating. However, unfavorable residual stresses in the composite system complicate good adhesion. Residual stresses in the coating and in the substrate affect the adhesive and cohesive damage processes at the coating-substrate interface that can either promote or prevent adhesion failure (6-12).

MATERIALS AND METHODOLOGY OF EXPERIMENT

To verify the effects of laser ablation prior to forming PVD coatings, two substrates (base materials) were used. HSS 6-5-2-5 tool steel used as the first substrate is characterized by good toughness, relatively higher wear resistance and very high tensile strength. Its hardness is ~66 HRC. The steel contains martensitic structure after heat treatment and carbides of the additive elements (MC , M_6C , $M_{23}C_6$). Another type of the base material was the WC-Co cemented carbide, designated as HB30. The cobalt matrix content is 10 wt. %. Microstructure of all substrates is shown in Fig. 1.

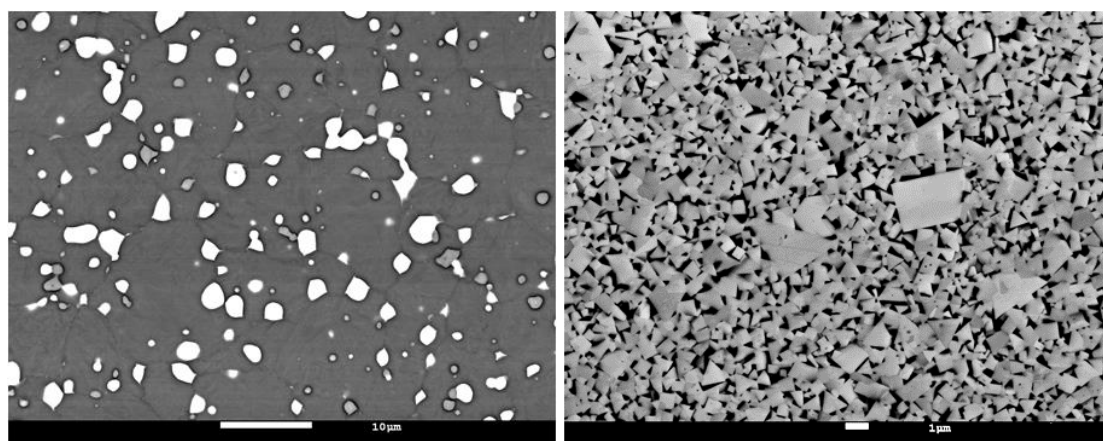


Fig. 1 Microstructure of the substrates a) HSS, b) WC-Co

In order to ensure good adhesion of the coatings to the base material, disc samples with a diameter of 12 mm x 4 mm prior to the evaporation process were polished with a Buehler Metadi 1 μm diamond suspension. RTG diffraction analysis measured the values of the surface

residual stress by means of the X-ray tensometric method $\sin^2\psi$ using a PanAlyticalEmpyrean X-ray diffractometer. To measure residual surface stresses, omega scans were used on selected high-angle crystallographic planes for substrates. Subsequently, the AVANTEK Company, s.r.o. Nové Mesto nad Váhom carried out laser ablation of both substrates by G4 PulsedFiber Laser, in a combination of three modes with different ablation parameters. These parameters are shown in Table 1. The affected area on the samples was 8x8 mm. After laser treatment, the values of residual stresses were measured again.

Table 1: Combination of laser ablation parameters						
Sample mode	v [mm/s]	P [W]	f [Hz]	Pulse		
				mJ	ns	kW
1A	1500	20 (50%)	30000	0.665	240	14
2A	1500	20 (50%)	76000	0.265	50	9
3A	1500	12 (30%)	76000	0.159	50	5.4

Determination of topography and surface roughness of substrates before and after laser ablation was performed by the ZEISS LSM 700 laser confocal microscope. A diode laser with a wavelength of 405 nm was used as a source of radiation.

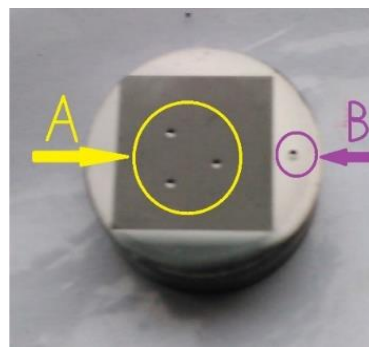


Fig. 2 A - indent in the treated area, B - indent in the non-treated area

The monolayer CrN coatings were deposited on the samples using the LARC[®] (Lateral Rotating Cathodes) process - vacuum arc evaporation with laterally rotating cathodes. The deposition process was carried out by the PLATIT π^{80} +DLC equipment, using one Cr cathode (99.99%). Deposition parameters were: Cr cathode current $I = 150$ A, substrate bias $U = -120$ V, substrate temperature $T = 450^\circ$ C, working pressure $p = 4$ Pa. Surface morphology of the substrates before and after laser ablation, as well as the morphology of the surfaces and character of the fracture areas of samples after the deposition process were observed by JEOL JSM 7600F high-resolution scanning electron microscope (SEM) in the secondary and backscattered electrons mode. The SEM parameters were: $U = 20$ keV, $I = 1$ nA and $WD = 15$ mm. The adhesion of the CrN coating to the base material was evaluated by a Mercedes test, using a Rockwell hardness tester with a load of 1500 N. The resulting indents were observed by SEM and compared with the standard etalons.

EXPERIMENTAL RESULTS

After laser treatment of the substrates surface (at different parameters), morphology changes were monitored by a scanning electron microscopy in secondary electron (LEI detector) mode. At first, were observed substrates after laser ablation in mode 1A. The surface

of the cemented carbide, after ablation, was formed by deep tracks in the direction of the laser beam (Fig. 3a). The distance of the edges from one to the other was approximately 50 μm . In addition, cracks were detected throughout the surface of the sample. The surface of the high-speed steel under the same parameters 1A (Table 1) is documented in Fig. 3b). In this case, the larger surface melting is clearly visible. Higher melting reduces the surface roughness. In case of 2A mode (Table 1), there was a significant change in surface layers. WC-Co (Fig. 3c) exhibited a different surface morphology, which was due to the higher frequency and lower laser beam width – a finer relief (the distance between edges is about 20 μm) with a higher number of cracks. The HSS in the same mode (Fig. 3d)) exhibits a smoother relief surface with the track's width approximately 22 μm . 3A mode differed in decreased laser power (12 W) and one pulse to 5.4 kW. The surface of the WC-Co is shown in Fig. 3e. The morphology is without laser beam tracks, but irregularly spaced hollows of different depths are visible. The entire surface is slightly wavy. Detected was also the presence of fine cracks. Using the same parameters (3A), Fig. 3f), local changes in surface morphology and smaller molten areas of different shapes were observed on the HSS substrates. On the surface, unmelted carbides can be observed.

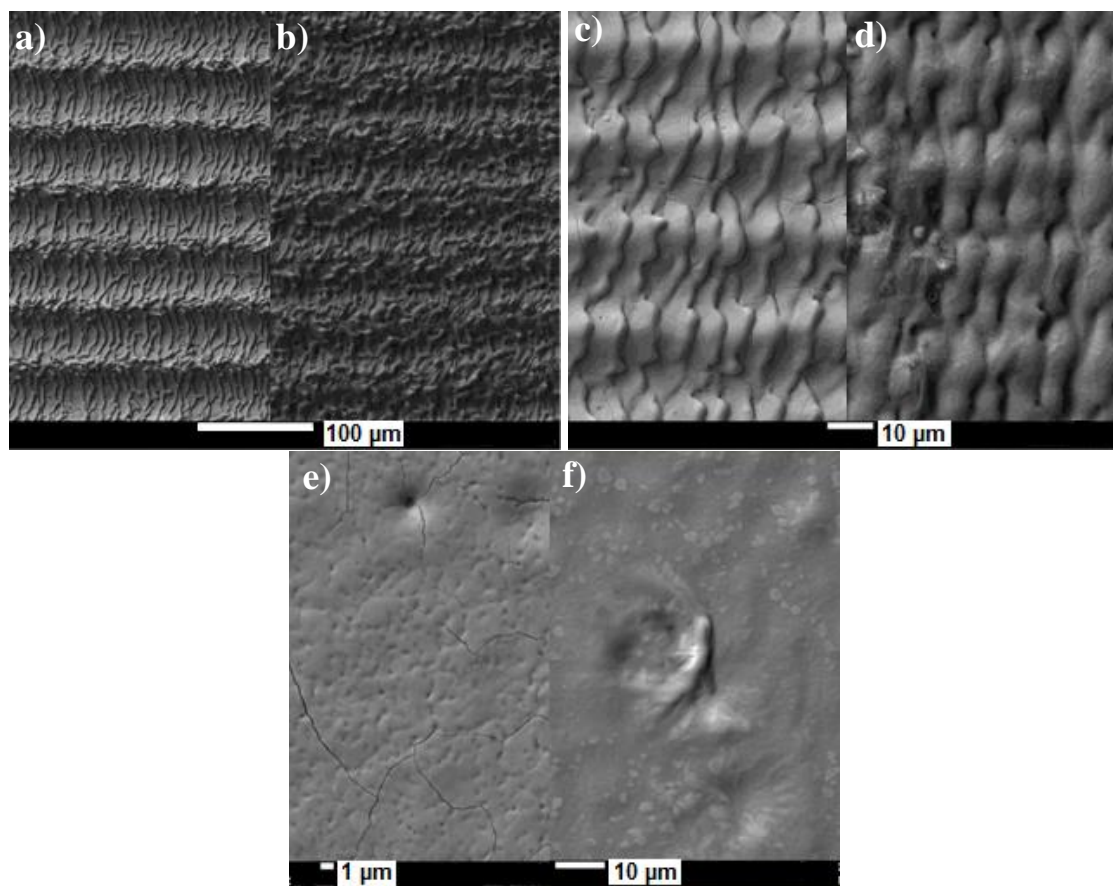


Fig. 3 a) Mode 1A WC-Co, b) Mode 1A HSS, c) Mode 2A WC-Co, d) Mode 2A HSS, e) Mode 3A WC-Co, f) Mode 3A HSS

After deposition of the CrN coating on the WC-Co substrate treated in 1A mode, the pale lines were observed (beam speed 1500 mm/s, pulse width 14 kW and frequency 3000 Hz) (Fig. 4a). This suggested the fact that the coating did not copy the morphology of the substrate. It is assumed that the CrN fills the deep tracks because the surface is relatively smooth. In the other case, the coating copied the morphology of the steel surface after laser ablation (1A), as shown in Fig. 4b). The surface of the cemented carbide affected by the 2A mode (beam speed 1500

mm.s-1, pulse output 9 kW and frequency 7600 Hz) is shown in Fig. 4c). Coating almost completely exterminates the surface of the molten base material. On the other hand, the CrN coating copied the HSS surface again and preserved the textured morphology. On the samples treated with a lower energy of laser radiation (3A), the coating behaved as follows: WC-Co + CrN surface, shown in Fig. 4e), was very similar, but of lower roughness. CrN on the HSS substrate accentuated the direction of the laser beam (Fig. 4f). This suggests that the coating is preferably formed at the micro-elevated sites of the substrate being affected.

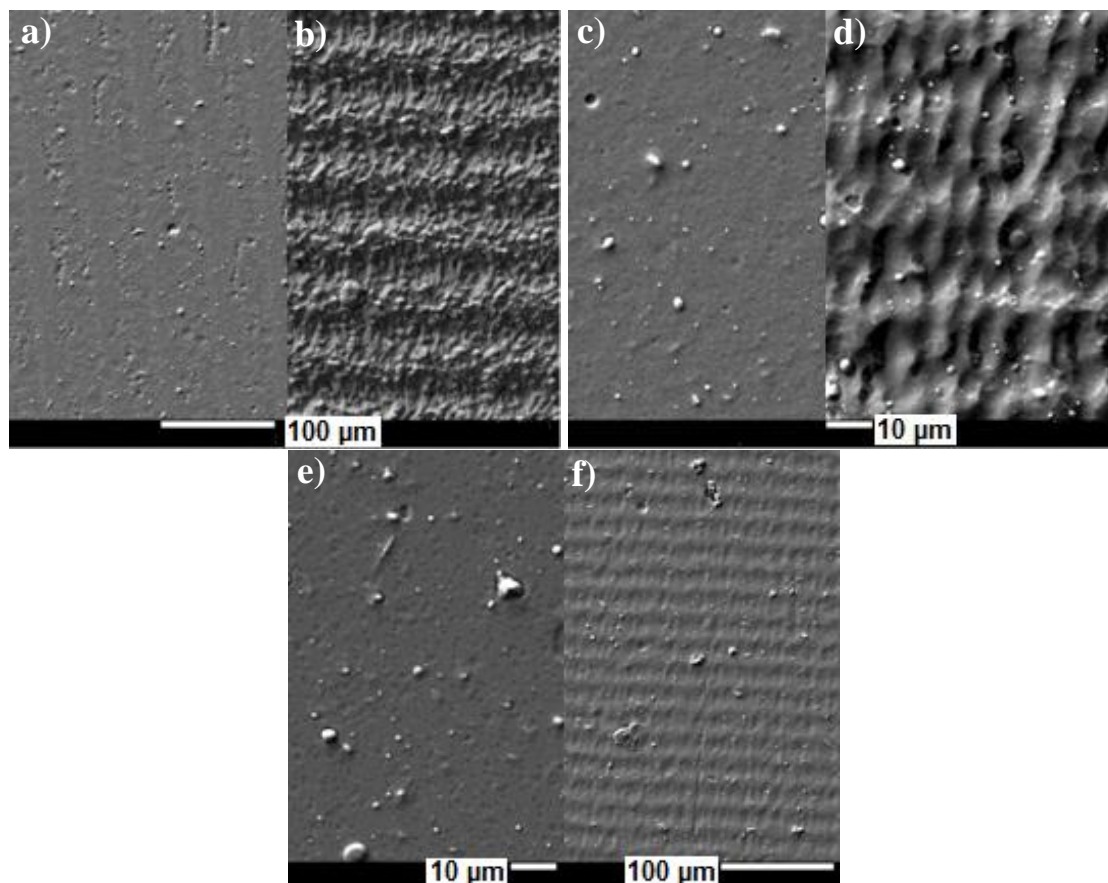


Fig.4 a) Mode 1A WC-Co + CrN, b) Mode 1A HSS + CrN, c) Mode 2A WC-Co + CrN, d) Mode 2A HSS + CrN, e) Mode 3A WC-Co + CrN, f) Mode 3A HSS + CrN

To compare the effect of laser ablation on the adhesion with adhesion on non-treated substrates, the Mercedes test was performed. Degree of the coating damage was assigned to both substrates without laser impact followed by evaluation of samples affected by laser ablation in modes 1A to 3A. The coating on the WC-Co substrate did not show the best adhesion, but it belonged to the group of acceptable (HF3) (Fig. 6a)). The coating on the steel substrate showed better adhesion and, according to the relevant damage, adhesion was included in the HF2 group (Fig. 5a)). After application of laser ablation on the surface of cemented carbide in mode 1A, the adhesion deteriorated (Fig. 6b)). The coating around the indent was considerably delaminated, so the adhesion was in the HF4 group. In the case of the coating to the HSS substrate, very good adhesion was observed. There were no peeled parts revealing the substrate around the indent. The Mercedes test performed on 2A WC-Co sample, differing from 1A in pulse rate and frequency, showed approximately the same degree of delamination. However, there was an increased incidence of deep cracks with a length of about 64.8 mm and more. Adhesion of the CrN coating to the steel (2A) surprisingly worsened (to an unacceptable

extent) even though the surface exhibited lower roughness. During the test, a large amount of coating was removed from the substrate around the indent. Size of the delaminated parts was about 100 μm , 168 μm max. In such a case, the coating-steel adhesion was worse than that of the coating-cemented carbide system.

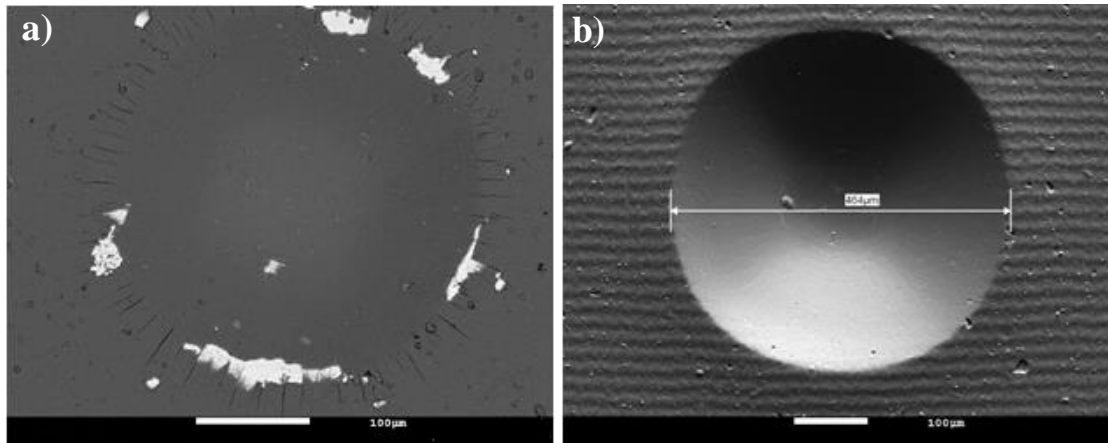


Fig. 5 a) Indent in the CrN coating deposited on the HSS surface without laser treatment, b) Indent in the CrN coating deposited on the HSS surface with laser treatment (3A)

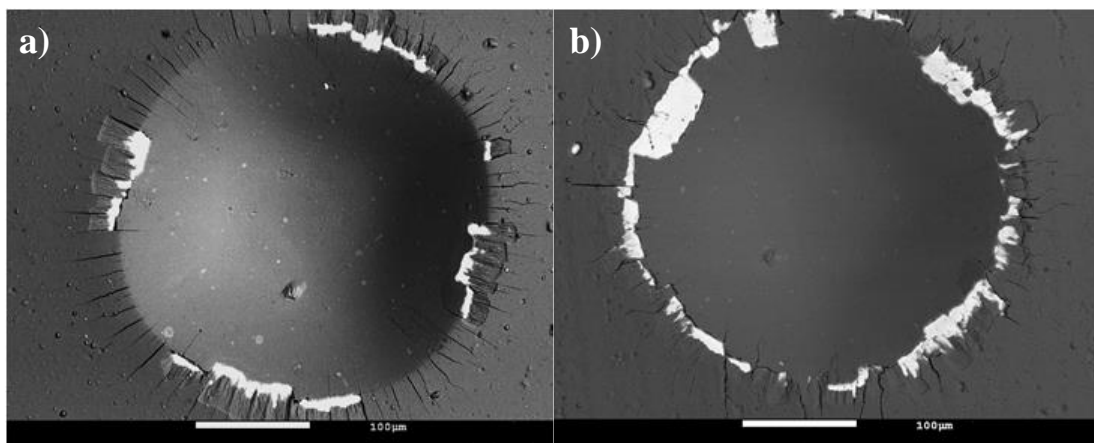


Fig. 6 a) Indent in the CrN coating deposited on the WC-Co surface without laser treatment, b) Indent in the CrN coating deposited on the WC-Co surface with laser treatment (1A)

The coating adhesion on the WC-Co substrate after 3A (HF2) ablation was much better than in the previous case. However, a slight delamination occurred. The number and size of the delaminated parts decreased. The incidence of cracks remained the same, with a slight reduction of their length of about 10 μm (compared to 2A). Changing one parameter of ablation (frequency) caused a huge improvement in adhesion of the coating-steel system (HF1) (Fig. 5b)). However, in a more detailed image, there are many small cracks spreading from the indent to the surroundings. Compared to the WC-Co samples, adhesion of the coating-steel (at 3A) improved by about one adhesion group. Roughness was analysed by laser confocal microscope using non-contact area analysis. All the measured roughness values (no ablation, ablation, post-deposition) are shown in Table 2. It is obvious how the roughness values were changed compared to the two substrates. While the roughness of the cemented carbides always decreased after coating deposition (in all cases - 1A, 2A, 3A), the steel roughness value of the coating

always increased after deposition. Differences in roughness before and after deposition are higher in 1A and 2A compared to 3A.

Laser ablation mode	R _{Sa} WC-Co [μm]	R _{Sa} WC-Co + CrN [μm]	R _{Sa} HSS [μm]	R _{Sa} HSS + CrN [μm]
No ablation	0.014	-	0.014	-
A1	2.16	0.15	2.34	2.63
A2	0.97	0.06	0.38	0.57
A3	0.10	0.05	0.12	0.15

Measurement for the presence of residual stresses using the RTG tensometric method $\sin^2\psi$ was performed on each sample four times on non-influenced substrates, on substrates after laser ablation (LA), on substrates after laser ablation with deposited coating (LA + CrN) and on the deposited coating. In all cases, samples were analyzed in two directions. Perpendicular to the direction of the laser beam (90) and in the direction of the laser beam (0). The measured values of the residual stresses of the WC-Co and the standard deviations (\pm) for each value are given in Table 3. The analysis of polished WC-Co substrates measured negative values of residual stresses (compressive stress) ranging from -330 to -45 MPa. After application of laser thermal treatment, all tensions were changed from the compressive to tensile (positive) values in the range of 670 to 1170 MPa. After application of the CrN coating, the residual stresses in the substrate remained positive. The greatest difference in residual stresses after application of the coating was recorded with 2A in the direction perpendicular to the beam direction (90), the value being reduced by 840 MPa. Compared to the residual stress values on the coated WC-Co samples with laser ablation, much lower stress values were measured in the samples with a CrN coating without thermal laser treatment.

Laser parameters	Direction of beam	Substrate WC-Co		With LA [MPa]		LA + CrN [MPa]		Without LA+ CrN [MPa]	
		WC-Co	\pm	[MPa]	\pm	[MPa]	\pm	[MPa]	\pm
1A	0	-70	25	900	80	1060	310	-1570	1360
	90	-60	20	1110	40	1170	360	-4600	810
2A	0	-210	40	1170	30	660	100	-3970	220
	90	-280	40	1120	50	280	60	-2520	740
3A	0	-80	30	900	40	660	110	-4980	1230
	90	-50	30	900	60	150	20	-5500	1190

Also, in the non-heat-treated substrates of HSS (after polishing), the compressive stress measured ranged from -1060 to -55 MPa (Table 4). When measuring the samples in two directions (0 and 90), the values were similar, the size varied at about 100 MPa. After application of laser ablation, the compressive stresses were changed to tensile ones varying at about 630 MPa (parameters 1A_0). After the deposition of CrN coating, the stresses decreased but remained tensile (except 1A). Differences in values were lower than those of the WC-Co samples. At 3A_0 samples the change was the smallest. The samples with CrN coatings were characterized by a reversal of the residual stresses, the biggest difference (decrease) was observed again at 1A_0, and at 3A_0 the change was minimal (this time also with the coating).

Table 4: Values of residual stresses on HSS samples

Laser parameters	Direction of beam	Substrate HSS	With LA		LA + CrN		Without LA+ CrN		
			±	[MPa]	±	[MPa]	±	[MPa]	
1A	0	-1060	70	630	170	-60	210	-5710	320
	90	-1100	80	230	180	-260	120	-2880	220
2A	0	-1010	70	510	155	30	80	-5350	610
	90	-305	60	520	160	140	70	-5650	470
3A	0	-55	110	170	80	170	60	-4290	1000
	90	-180	90	540	100	250	80	-4910	110

DISCUSSION

During the initial analysis of polished non-treated substrates after coating deposition, both samples exhibited compressive stress and ideal roughness (0.014 μm). The samples of WC-Co exhibited reduced adhesion with peeling of more than two-thirds of the coating at the edges of the indented regions. The samples of HSS exhibited suitable adhesion with small delamination between cracks. After applying the modes of different ablation parameters, these characteristics changed. Residual stresses changed to the tensile ones after thermal treatment, and this fact did not change in most cases even after the coating had been deposited. Substrate surface morphology, melting depth, roughness and adhesion varied depending on the ablation mode used. In the case of WC-Co substrate, mode 1A caused melting of the surface to the depth of about 1 μm . The laser beam formed deep tracks on the surface, which was accompanied by cracks propagation. After application of the coating, the morphology was relatively smoothed, although the presence of microparticles was detected on the surface. Adhesion decreased. After applying the mode 2A, fine lines appeared instead of deep tracks, but more cracks appeared. After deposition of CrN, observed was complete surface smoothing with lower amount of microparticles. The fracture area showed melting to the depth up to 0.41 μm , and adhesion was considered as reduced in the same way as in the previous case. After the 3A ablation, the melting of the surface remained roughly the same. Analysis showed only a fine wavy surface with the presence of pores. After application of 3A mode, adhesion was satisfactory, with small delamination around the indents (HF2). Roughness increased after all modes (the highest value at 1A = 2.166 μm), but after deposition of the coating, it dropped by at least half and more. The lowest roughness after CrN deposition was 0.05 μm (after 3A mode). Neves et al. evaluated the effectiveness of laser texturing in improving the substrate–coating adhesion of PVD coated cemented carbide. The WC-Co substrates were textured using a Nd:YAG laser and different parameters (four different intensities), and then coated with TiAlN monolayer. In that case, also the sample after laser ablation showed better performance in the indentation and turning tests than the standard samples. Anchoring provided by the higher roughness of the textured surface increased the adhesion of the coating to the substrate, thus increasing the tool life [10]. Fang et al. found that ablation increases proportionally with the pulse number and the energy applied. The laser affected zone is covered by a very thin recast layer and the laser-induced defects (such as pores and micro-cracks) were only found at the subsurface. The structure is quite brittle and porous, becoming more pronounced when the applied laser pulse increases [9].

After application of laser ablation in 1A mode on HSS, its surface melted most of all (7.71 μm). After its deposition, the coating copied the tracks that had appeared on the surface. The adhesion was satisfactory (HF2). After 2A mode, less melting was found (2.39 μm). The steel exhibited less roughness, the deposited coating retained rugged morphology, but the adhesion

significantly deteriorated to an unacceptable level (HF6). After ablation 3A, the steel surface was melting to 1 μm depth. After laser ablation, the almost smooth surface changes after deposition of the coating. It was not smooth, but the direction of laser beam transition on the sample was more expressed; fine lines appeared. Adhesion tests showed very good adhesion (HF1) with an unimportant number of small cracks. One explanation for this enhanced adhesion of the textured surface compared with the standard ones is the mechanical anchoring of the coating provided by the texturing process. The roughness analysis revealed the opposite phenomenon compared to the WC-Co samples. Values of roughness increased after laser ablation (all modes) (this increase was more pronounced than in WC-Co). Deposition of the coating did not decrease the values, but it increased the roughness. The values ranged from 0.15 to 2.627 μm . This leads to the assumption that the textured surface of the base materials acts as a barrier against the slipping of the coating, while increasing the adhesion between the coating and the substrate. Moreover, rougher surface provides a larger area of contact with the coating, since its material might penetrate into the roughness tracks after the laser beam.

CONCLUSION

The contribution deals with the analysis of the influence of the substrate surface laser ablation before deposition process to improve the adhesion of the coating-substrate system. The CrN coating was applied to the HSS 6-5-2-5 (STN 19 852) and the WC-Co HB30 cemented carbide with cobalt content of 10 wt%. The laser ablation was carried out on both substrates by pulse laser of G4 PulsedFiber Laser, using a combination of three modes of different ablation parameters. The influence of laser ablation of substrate surface on the substrate morphology, structure, roughness, presence of residual stresses inside the substrates and layers as well as their adhesion behavior between the layers and the base material was studied. Based on the results of these experiments, it can be concluded that:

- Laser ablation had an influence on the substrate's morphology (textured and remelted surface);
- Significant presence of cracks was observed on the surface of the WC-Co;
- Surface roughness increased after laser ablation owing to texturing;
- Roughness of the cemented carbide substrate decreased after the coating deposition, and, in the case of the steel substrate, increased roughness was detected;
- Adhesion was dependent on the laser power and frequency. The best adhesion was observed in the case of steel effected by the lowest power;
- Change in the character of residual stresses in substrates from compressive to tensile was observed after the substrates' laser processing.

References:

1. KRIŽAN, L., GRGAČ, P., ČAPLOVIČ, L. 1988. *Special Technology I. Progressive methods of heat treatment*. Bratislava: SVŠT, pp.270-291. ISBN 8022701920.
2. CAVALEIRO, A., T. DE HOSSON, J. 2007. *Nanostructured Coatings*. Canada: Springer, p. 7. ISBN-13: 978-0387256429.
3. ANTONOV, M., HUSSAINOVA, I., SERGEJEV, F., KULU, P., GREGOR, A. 2009. Assessment of gradient and nanogradient PVD coatings behavior under erosive, abrasive and impact wear conditions. In *Wear*, **267**(5 – 8), pp. 898 – 906. ISSN: 0043-1648.
4. VOJS, M., MARTON, M. 2014. Diamond coatings. In *TriboTechnika*, **6**(1), pp. 44-46. ISSN 1338-0524.
5. ADAMIÁK, M., DOBRZAŃSKI, Leszek A. 2008. Microstructure and selected properties of hot-work tool steel with PVD coatings after laser surface treatment. In *Applied Surface Science*.

- Institute of Engineering Materials and Biomaterials, Silesian University of Technology, 44-100 Gliwice, Konarskiego Street 18A, pp. 4552–4556.
6. BODZIN, K., BRÖGELMANN, T., GILLNER, A., KRUPPE, N. C., HE, C., NADERI, M. 2018. Laser-structured high performance PVD coatings. In *Surface and Coatings Technology*, Vol. 352, pp. 302-312.
 7. BOBZIN, K., HOPMANN, C.H., GILLNER, A., BRÖGELMANN, T., KRUPPE, N.C., ORTH, M., STEGER, M., NADERI, M. 2017. Enhanced replication ratio of injection molded plastic parts by using an innovative combination of laser-structuring and PVD coating. In *Surface and Coatings Technology*. Vol. 332, pp. 474-483.
 8. BOBZIN, K., BRÖGELMANN, T., KRUPPE, N.C. 2018. Enhanced PVD process control by online substrate temperature measurement. In *Surface and Coatings Technology*. Vol. 354, pp. 383-389.
 9. FANG, S., LIMA, R., SANDOVAL, D., BÄHRE, D., LLANES, L. 2018. Ablation Investigation of Cemented Carbides Using Short Pulse Laser Beams. In *Science Direct*, 19th CIRP Conference on Electro Physical and Chemical Machining, Bilbao, Spain.
 10. NEVES, D., DINIZ, A. E., LIMA, M. S. F. 2013. Microstructural analyses and wear behavior of the cemented carbide tools after laser surface treatment and PVD coating. In *Applied Surface Science*. Vol. 282, pp. 680-688.
 11. FU, Y., HU, J., HUO, W., CAO, W., ZHANG, R., ZHAO, W. 2018. Characterization of high-current pulsed electron beam interaction with AISI 1045 steel and the microstructure evolution. In *Science Direct*, 19th CIRP Conference on Electro Physical and Chemical Machining, Bilbao, Spain.
 12. VILLERIUS, V., KOOIKER, H., POST, J., PEI, Y. T. 2019. Ultrashort pulsed laser ablation of stainless steels. In *International Journal of Machine Tools and Manufacture*. Vol. 138, pp. 27 – 35.

ORCID:

Lubomír Čaplovič 0000-0002-2280-008